Optimization of sawtooth surface-relief gratings: effects of substrate refractive index and polarization

Shun-Der Wu, Thomas K. Gaylord, and Elias N. Glytsis

The effect of the refractive index of the substrate together with the incident polarization on the optimization of sawtooth surface-relief gratings (SRGs) is investigated. The global optimum diffraction efficiencies of the −1st forward-diffracted order of sawtooth SRGs are 63.3% occurring at $n_2 = 1.47$ for TE polarization and 73.8% occurring at $n_2 = 2.88$ for TM polarization. Incident TE polarization has higher optimum diffraction efficiency than TM polarization for all $n_2 < 1.85$. In contrast, TM polarization has higher optimum diffraction efficiency than TE polarization for all $n_2 > 1.85$. A polymer ($n_2 = 1.5$) optimum sawtooth SRG exhibits 62.6% efficiency for TE polarization. A silicon ($n_2 = 3.475$) optimum sawtooth SRG exhibits 68.6% efficiency for TM polarization. These sawtooth SRGs are compared to right-angle-face trapezoidal SRGs. It is found that the optimum profiles of right-angle-face trapezoidal SRGs have only very slightly increased efficiencies over sawtooth SRGs (0.04% for TE and 0.55% for TM). © 2006 Optical Society of America

OCIS codes: 050.0050, 050.1950, 230.1950, 260.5430.

1. Introduction

Surface-relief gratings (SRGs) are of great interest owing to their various applications such as disk pick-up heads,[1,2] optical sensors,[3,4] guided-mode resonant filters,[5–7] beam splitters,[8] reflectors,[9,10] and couplers for optical interconnects.[11,12] SRGs can be fabricated in photoresist using optical interferometry in conjunction with reactive-ion etching,[10] fabricated with a silicon (Si) mold using nanoimprint lithography,[13] or fabricated with direct-writing electron-beam lithography.[14] In order to utilize these technologies to fabricate SRGs in demanding applications, the optimization of SRGs is critically important.

For the optimum design of SRGs, Moharam and Gaylord[15] used the rigorous coupled-wave analysis (RCWA) to investigate the diffraction characteristics of sinusoidal, square-wave, triangular, and sawtooth SRGs with respect to groove depths for TE polarization incident at a first Bragg angle of 30 degrees. The optimum groove depths for various SRG profiles were presented. Yokomori[16] applied a differential method to investigate the diffraction characteristics, and therefore, to determine the optimum groove depths of sinusoidal, rectangular, and triangular SRGs for both TE and TM polarizations incident at a first Bragg angle of 45 degrees. Gupta and Peng[17] presented both theoretical analyses (based on the modal method) and experimental results of the optimum designs of groove depths for rectangular SRGs. Furthermore, Gerritsen and Jepsen[18] used the RCWA to determine the optimum filling factors and the corresponding optimum groove depths of rectangular SRGs for randomly polarized light incident at first Bragg angles of 30, 37.5, and 45 degrees. In all of these designs, the optimum profiles of SRGs were determined by varying one grating parameter and fixing the others instead of optimizing all grating parameters simultaneously. Furthermore, the substrates used in these analyses were focused on polymers whose refractive indices ranged from $n_2 = 1.2$ to $n_2 = 2.0$.

Recently, Wu *et al.*[19] applied the simulated annealing (SA) algorithm in conjunction with the RCWA to optimize simultaneously the groove depth d, the top filling factor F_1, and the bottom filling factor F_2 of anisotropically etched Si SRGs ($n_2 = 3.475$) normally illuminated by both TE-polarized and TM-polarized light to provide a 45-degree diffracted angle of the −1st forward-diffracted order. A number of results emerged from this investigation. For example, the TE-optimized profile has a pointed top and a flat bottom. In contrast, the TM-optimized profile has a

S.-D. Wu and T. K. Gaylord (tgaylord@ece.gatech.edu) are with the School of Electrical and Computer Engineering, Microelectronics Research Center, Georgia Institute of Technology, Atlanta, Georgia 30332. E. N. Glytsis is with the School of Electrical and Computer Engineering, the National Technical University of Athens, Greece.

Received 6 July 2005; revised 22 December 2005; accepted 30 December 2005; posted 4 January 2005 (Doc. ID 63166).

0003-6935/06/153420-05$15.00/0

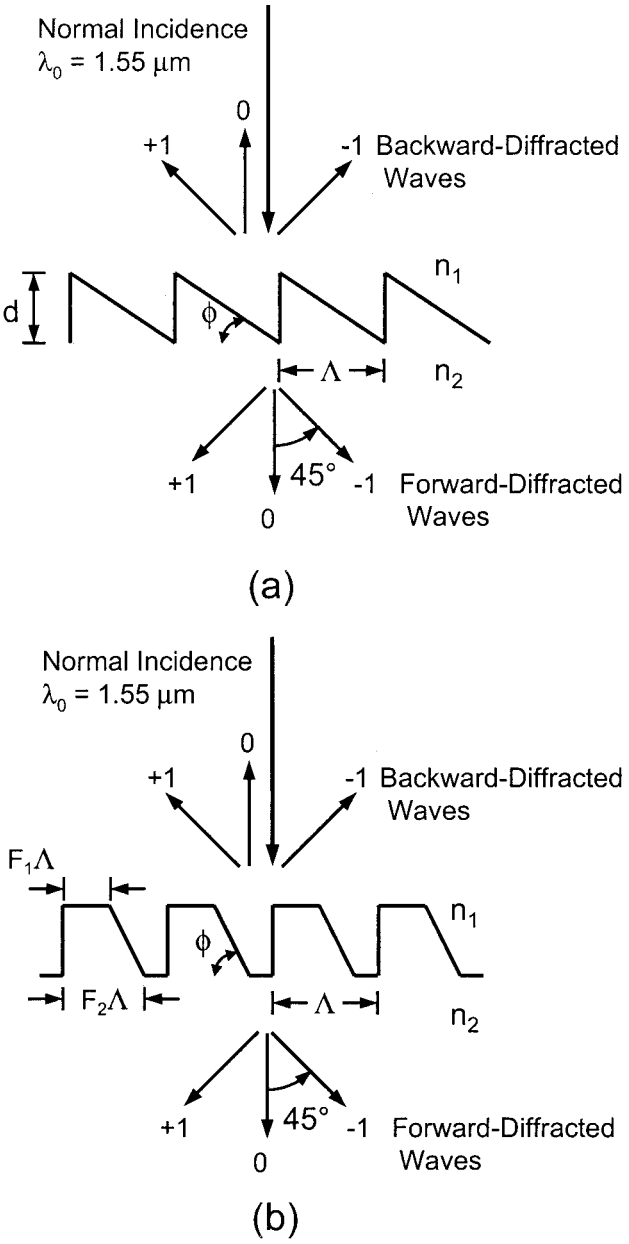

Fig. 1. Configurations of (a) a sawtooth SRG and (b) a right-angle-face trapezoidal SRG illuminated by a normally incident plane wave with free space wavelength $\lambda_0 = 1.55$ μm. The refractive indices of the incident region and the substrate are n_1 and n_2, respectively. The SRGs are characterized by the grating period Λ (designed for 45-degree forward-diffracted angle of the -1st forward-diffracted order), the groove depth d, the top filling factor F_1, the bottom filling factor F_2, and the slant angle ϕ.

flat top and a pointed bottom. In addition, the optimum diffraction efficiency of TM polarization is 67.1%, which is much higher than that of TE polarization (37.3%). However, the effects of substrate index and polarization taken together are not well understood. In this paper, the optimum groove depths and the corresponding diffraction efficiencies of sawtooth SRGs [i.e., $F_1 = 0$ and $F_2 = 1$ in Fig. 1(a)] with respect to the refractive indices of substrates for both TE and TM polarizations are determined by applying the RCWA. Furthermore, the optimum profiles of sawtooth SRGs are compared to those of right-angle-face trapezoidal SRGs [i.e., $F_1, F_2,$ and ϕ are varied in Fig. 1(b)], which is determined by using the SA algorithm[19–21] in conjunction with the RCWA,[19] both in polymer ($n_2 = 1.5$) and in Si ($n_2 = 3.475$).

2. Sawtooth Grating Diffraction

The general right-angle-face trapezoidal SRG, characterized by the grating period Λ, the groove depth d, the top filling factor F_1, the bottom filling factor F_2, and the slant angle ϕ, is shown in Fig. 1(b). It is noted that a sawtooth SRG shown in Fig. 1(a) is a special case of the right-angle-face trapezoidal SRG with $F_1 = 0$ and $F_2 = 1$. As shown in Fig. 1, a plane wave with free space wavelength $\lambda_0 = 1.55$ μm in air with refractive index $n_1 = 1.0$ is normally incident upon the SRG with refractive index n_2 producing both forward-diffracted and backward-diffracted waves. The substrate material also has a refractive index of n_2. The grating period is designed to provide 45-degree forward-diffracted angle of the -1st propagation order and is given by $\Lambda = \lambda_0/n_2 \sin 45°$. Normal incidence and diffraction at a 45-degree forward-diffracted angle represents a canonical configuration used for substrate-mode optical interconnects and similar applications. Thus, in this work, the angle of diffraction remains fixed. Therefore the period varies inversely with n_2. Therefore, there are three forward-diffracted orders (the -1st, the 0th, and the $+1$st orders). However, depending on the refractive index of the substrate, there are three backward-diffracted orders (the -1st, the 0th, and the $+1$st orders) if $n_2 < \sqrt{2}$, and only the 0th backward-diffracted order exists (i.e., the ± 1st backward-diffracted orders are cut off) if $n_2 \geq \sqrt{2}$.

For the optimization of a sawtooth SRG, since the grating parameters of $\Lambda = \lambda_0/n_2 \sin 45°$, $F_1 = 0$, and $F_2 = 1$ are specified, the RCWA is utilized to determine the optimum groove depth d_{opt} by varying the groove depth, and therefore, to obtain the corresponding optimum slant angle $\phi_{\text{opt}} = \tan^{-1}(d_{\text{opt}}/\Lambda)$. On the other hand, for the optimization of a right-angle-face trapezoidal SRG in a polymer ($n_2 = 1.5$) or in Si ($n_2 = 3.475$), the SA in conjunction with the RCWA is applied to optimize the grating parameters of $d, F_1, F_2,$ and ϕ systematically and simultaneously.

3. Optimized Surface-Relief Gratings

A. Sawtooth Surface-Relief Gratings

Figure 2 shows the optimum diffraction efficiencies of the -1st forward-diffracted order $\text{DE}_{-1,\text{opt}}{}^{\text{T}}$ of a sawtooth SRG ($F_1 = 0$ and $F_2 = 1$) for both TE and TM polarizations as a function of the refractive index of the substrate n_2. The corresponding characteristics of optimum diffraction efficiencies for a volume grating (VG) (with planar parallel surfaces) as a function of the average refractive index of the VG(n_2) are also presented in Fig. 2. Similar to the sawtooth SRG,

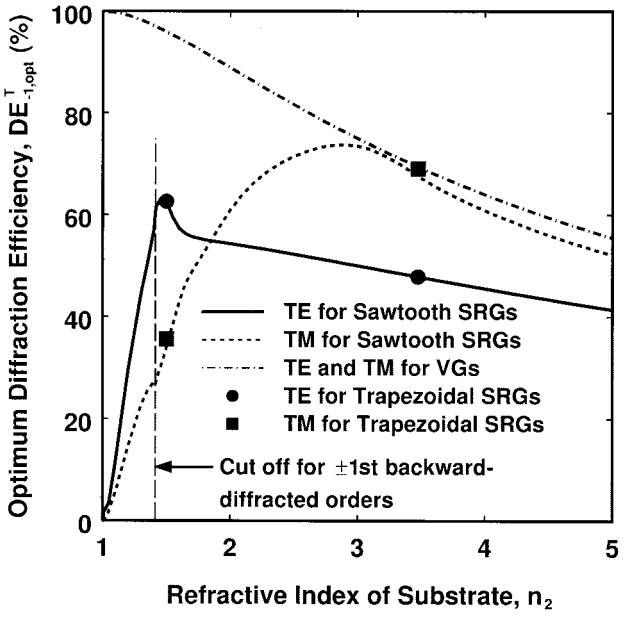

Fig. 2. Optimum diffraction efficiencies of the −1st forward-diffracted order for both a sawtooth SRG and a VG as a function of n_2 for both TE and TM polarizations. The corresponding optimum diffraction efficiencies of a right-angle-face trapezoidal SRG in a polymer ($n_2 = 1.5$) and in Si ($n_2 = 3.475$) for both TE and TM polarizations are denoted by solid circles (●) and solid squares (■), respectively.

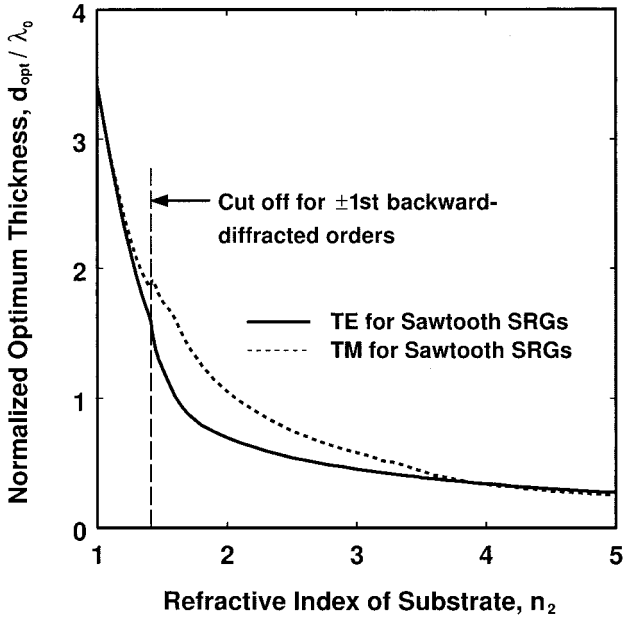

Fig. 3. Normalized optimum thickness of a sawtooth SRG as a function of n_2 for both TE and TM polarizations.

the VG is designed to provide 45-degree forward-diffracted angle of the −1st propagation order. The refractive-index modulation of the VG is assumed to be $\Delta n = 0.01\, n_2$.

As shown in Fig. 2, the optimum diffraction efficiencies of a VG for both TE and TM polarizations are very close to each other and decrease monotonically as the average refractive index of the VG(n_2) increases. The behaviors of $DE_{-1,opt}{}^{T}$ of a VG for both TE and TM polarizations can be approximated by $DE_{-1,opt}{}^{T} \approx (1 - R) \times 100\%$, where $R = [(1 - n_2)/(1 + n_2)]^2$ is the fraction of power reflected (reflectance) for a planar interface comprised of air (with refractive index 1.0) and a VG (with average refractive index n_2). As a result, the optimum diffraction efficiencies of a VG for both TE and TM polarizations can achieve $DE_{-1,opt}{}^{T,TE} = DE_{-1,opt}{}^{T,TM} = 99.99\%$, which are close to 100%, as n_2 decreases to 1.0. Although not treated here, an appropriate anti-reflection coating can be added to a VG, allowing the diffraction efficiency to approach 100% for any given substrate index n_2. However, in contrast to a VG, $DE_{-1,opt}{}^{T}$ of a sawtooth SRG for TE polarization increases as n_2 increases and reaches the maximum of $DE_{-1,opt,max}{}^{T,TE} = 63.32\%$ at $n_2 = 1.47$, where the corresponding $DE_{-1,opt}{}^{T}$ for TM polarization is $DE_{-1,opt}{}^{T,TM} = 31.38\%$, and decreases monotonically as n_2 increases further ($n_2 > 1.47$). On the other hand, $DE_{-1,opt}{}^{T}$ of a sawtooth SRG for TM polarization increases at a slow rate as n_2 increases and reaches the maximum of $DE_{-1,opt,max}{}^{T,TM} = 73.76\%$ at $n_2 = 2.88$, where the corresponding $DE_{-1,opt}{}^{T}$ for TE polarization is $DE_{-1,opt}{}^{T,TE} = 50.60\%$, and decreases monotonically as n_2 increases further ($n_2 > 2.88$). It is noted that there is a local minimum of $DE_{-1,opt}{}^{T,TM}$ at $n_2 = \sqrt{2}$. This occurs due to the ±1st backward-diffracted orders being cut off at $n_2 = \sqrt{2}$. In addition, the maximum difference between $DE_{-1,opt}{}^{T,TE}$ and $DE_{-1,opt}{}^{T,TM}$ is $(DE_{-1,opt}{}^{T,TE} - DE_{-1,opt}{}^{T,TM})_{max} = 33.19\%$ at $n_2 = 1.45$ and $(DE_{-1,opt}{}^{T,TM} - DE_{-1,opt}{}^{T,TE})_{max} = 23.44\%$ at $n_2 = 3.00$. Consequently, for sawtooth SRGs with small refractive indices ($n_2 < 1.85$) such as polymer sawtooth SRGs, the optimum performance of TE polarization is better than that of TM polarization. However, for sawtooth SRGs with high refractive indices ($n_2 > 1.85$) such as semiconductor sawtooth SRGs, the optimum performance of TM polarization is better than that of TE polarization. Finally, for both TE and TM polarizations, the optimum diffraction efficiencies of a sawtooth SRG approach those of a VG as $n_2 \gg 1.0$. For example, for $n_2 = 10$, the optimum diffraction efficiencies of a sawtooth SRG for both TE and TM polarizations are $DE_{-1,opt}{}^{T,TE} = 27.67\%$ and $DE_{-1,opt}{}^{T,TM} = 32.14\%$, respectively, and these are close to those of a VG with $DE_{-1,opt}{}^{T,TE} = DE_{-1,opt}{}^{T,TM} = 33.06\%$.

Figures 3 and 4 show the interrelated normalized optimum thickness d_{opt}/λ_0 and the optimum slant angle ϕ_{opt} of a sawtooth SRG as a function of n_2. As shown in Fig. 3, for TE polarization, d_{opt}/λ_0 decreases monotonically as n_2 increases. However, for TM polarization, d_{opt}/λ_0 decreases as n_2 increases from $n_2 = 1.0$ to $n_2 = \sqrt{2}$, increases slightly as n_2 increases from $n_2 = \sqrt{2}$ to $n_2 = 1.42$ owing to the cutoff of the ±1st backward-diffracted orders, and then decreases

Table 1. Optimization of both Sawtooth SRGs and Right-Angle-Face Trapezoidal SRGs in Polymers (n_2 = 1.5) and in Si (n_2 = 3.475) for TE and TM Polarizations

Sawtooth SRGs (F_1 = 0 and F_2 = 1)				
Optimized Parameters	Polymers (n_2 = 1.5)		Si (n_2 = 3.475)	
	TE	TM	TE	TM
d_{opt} (μm)	1.913	2.710	0.606	0.723
ϕ_{opt} (deg)	52.624	61.664	43.851	48.906
$DE_{-1,opt}{}^{T}$ (%)	62.573	33.944	47.867	68.547
Right-Angle-Face Trapezoidal SRGs (F_1, F_2, and ϕ are varied)				
Optimized Parameters	Polymers (n_2 = 1.5)		Si (n_2 = 3.475)	
	TE	TM	TE	TM
d_{opt} (μm)	1.848	2.006	0.601	0.484
ϕ_{opt} (deg)	52.863	65.345	43.868	64.150
$F_{1,opt}$	0.040	0.271	0.000	0.517
$F_{2,opt}$	0.998	0.901	0.992	0.889
$DE_{-1,opt}{}^{T}$ (%)	62.612	35.682	47.869	69.093

monotonically as n_2 increases further ($n_2 > 1.42$). On the other hand, ϕ_{opt} for TE polarization decreases as n_2 increases (shown in Fig. 4). By comparison, ϕ_{opt} for TM polarization decreases slowly as n_2 increases. For both TE and TM polarizations, the normalized optimum thicknesses and optimum slant angles approach $d_{opt}/\lambda_0 = 0$ and $\phi_{opt} = 45°$, respectively, as $n_2 \gg 1.0$. It is worth mentioning that the normalized optimum thicknesses of VGs are almost constants and are in the ranges of $41.94 < d_{opt}/\lambda_0 < 42.14$ for TE polarization and $59.37 < d_{opt}/\lambda_0 < 59.55$ for TM polarization. Furthermore, the slant angles of VGs are fixed to be $\phi = 67.5°$.

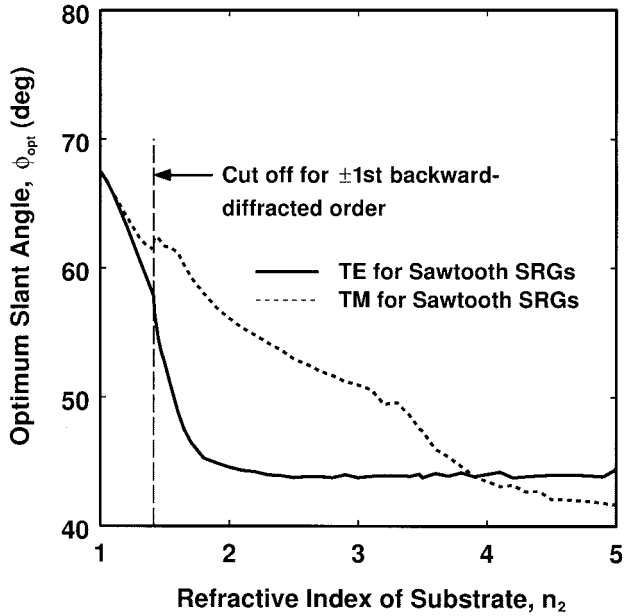

Fig. 4. Optimum slant angle of a sawtooth SRG as a function of n_2 for both TE and TM polarizations.

B. Right-Angle-Face Trapezoidal Surface-Relief Gratings

Table 1 summarizes the optimized grating parameters of both sawtooth SRGs (F_1 = 0 and F_2 = 1) and right-angle-face trapezoidal SRGs (F_1, F_2, and ϕ are varied) both in polymers (n_2 = 1.5) and in Si (n_2 = 3.475) for both TE and TM polarizations. The corresponding $DE_{-1,opt}{}^{T}$ of right-angle-face trapezoidal SRGs in n_2 = 1.5 and in n_2 = 3.475 for both TE polarization (denoted by solid circles) and TM polarization (denoted by solid squares) are also represented in Fig. 2. As shown in Table 1, for TE polarization, the optimum filling factors of right-angle-face trapezoidal SRGs for polymers are $F_{1,opt}$ = 0.040 and $F_{2,opt}$ = 0.998 and for Si are $F_{1,opt}$ = 0.000 and $F_{2,opt}$ = 0.992, and both are close to those of sawtooth SRGs (F_1 = 0 and F_1 = 1). In other words, the optimum grating profiles of right-angle-face trapezoidal SRGs closely resemble those of sawtooth SRGs for TE polarization. However, for TM polarization, the optimum filling factors of right-angle-face trapezoidal SRGs for polymers are $F_{1,opt}$ = 0.271 and $F_{2,opt}$ = 0.901 and for Si are $F_{1,opt}$ = 0.517 and $F_{2,opt}$ = 0.889, which are quite different from those of sawtooth SRGs. Therefore, due to these nonzero $F_{1,opt}$, the optimum grating profiles of right-angle-face trapezoidal SRGs for TM polarization possess flat tops, higher slant angles, and smaller groove depths with respect to those of sawtooth SRGs. Furthermore, for n_2 = 1.5 (polymer SRGs), the optimum diffraction efficiencies for TE polarization are $DE_{-1,opt}{}^{T,TE}$ = 62.57% for a sawtooth SRG and $DE_{-1,opt}{}^{T,TE}$ = 62.61% for a right-angle-face trapezoidal SRG. These are much higher than those of TM polarization for which $DE_{-1,opt}{}^{T,TM}$ = 33.94% for a sawtooth SRG and $DE_{-1,opt}{}^{T,TM}$ = 35.68% for a right-angle-face trapezoidal SRG. However, for n_2 = 3.475 (Si SRGs), the optimum diffraction efficiencies of TM polarization are $DE_{-1,opt}{}^{T,TM}$ = 68.55% for a sawtooth SRG and $DE_{-1,opt}{}^{T,TM}$ = 69.09% for a right-angle-face trapezoidal SRG. These diffraction efficiencies are much higher than those of TE polarization for which $DE_{-1,opt}{}^{T,TE}$ = 47.87% for a sawtooth SRG and $DE_{-1,opt}{}^{T,TE}$ = 47.87% for a right-angle-face trapezoidal SRG.

4. Summary and Discussion

In this paper, the effects of the substrate refractive index (n_2) and the incident polarization on the optimization of sawtooth SRGs were investigated and compared with VGs and right-angle-face trapezoidal SRGs. The global optimum diffraction efficiencies for sawtooth SRGs are $DE_{-1,opt,max}{}^{T,TE}$ = 63.32% occurring at n_2 = 1.47 for TE polarization and are $DE_{-1,opt,max}{}^{T,TM}$ = 73.76% occurring at n_2 = 2.88 for TM polarization. For all $n_2 < 1.85$, the optimum diffraction efficiency of TE polarization is higher than that of TM polarization. However, the optimum dif-

fraction efficiency of TM polarization is higher than that of TE polarization for all $n_2 > 1.85$. Consequently, TE polarization is suggested to be used for the optimization of polymer SRGs (such as DuPont OmniDex photopolymers with $n_2 = 1.5$), and TM polarization is suggested to be used for the optimization of semiconductor SRGs (such as Si with $n_2 = 3.475$). Furthermore, for a large n_2, the optimum diffraction efficiencies of sawtooth SRGs for both TE and TM polarizations approach that of VGs, which is accurately predicted to be $(1 - R) \times 100\%$, where R is the reflectance of a single planar interface. On the other hand, the optimum profiles of right-angle-face trapezoidal SRGs in polymers with $n_2 = 1.5$ and in Si with $n_2 = 3.475$ determined by the SA in conjunction with the RCWA were compared to those of sawtooth SRGs. For TE polarization, the optimum profiles of right-angle-face trapezoidal SRGs resemble those of sawtooth SRGs, i.e., the optimum top filling factors and the optimum bottom filling factors of right-angle-face trapezoidal SRGs are close to $F_{1,\mathrm{opt}} = 0$ and $F_{2,\mathrm{opt}} = 1$, respectively. In contrast to TE polarization, the optimum profiles of right-angle-face trapezoidal SRGs for TM polarization possess flat tops (i.e., the optimum top filling factors are $F_{1,\mathrm{opt}} > 0$).

This research was performed as part of the Interconnect Focus Center (IFC) research program supported by the Semiconductor Research Corporation (SRC), the Microelectronics Advanced Research Corporation (MARCO), and the Defense Advanced Research Projects Agency (DARPA).

References

1. S. Ura, T. Suhara, H. Nishihara, and J. Koyama, "An integrated-optic disk pickup device," J. Lightwave Technol. **4,** 913–918 (1986).
2. T. Suhara and H. Nishihara, "Integrated optics components and devices using periodic structures," IEEE J. Quantum Electron. **22,** 845–867 (1986).
3. J. Dübendorfer and R. E. Kunz, "Compact integrated optical immunosensor using replicated chirped grating coupler sensor chips," Appl. Opt. **37,** 1890–1894 (1998).
4. M. Wiki and R. E. Kunz, "Wavelength-interrogated optical sensor for biochemical applications," Opt. Lett. **25,** 463–465 (2000).
5. D. L. Brundrett, E. N. Glytsis, and T. K. Gaylord, "Normal-incidence guided-mode resonant grating filters: design and experimental demonstration," Opt. Lett. **23,** 700–702 (1998).
6. Z. Hegedus and R. Netterfield, "Low sideband guided-mode resonant filter," Appl. Opt. **39,** 1469–1473 (2000).
7. S. Tibuleac and R. Magnusson, "Narrow-linewidth bandpass filters with diffractive thin-film layers," Opt. Lett. **26,** 584–586 (2001).
8. N. Rajkumar and J. N. McMullin, "V-groove gratings on silicon for infrared beam splitting," Appl. Opt. **34,** 2556–2559 (1995).
9. S. Hava and M. Auslender, "Silicon grating-based mirror for 1.3-μm polarized beams: MATLAB-aided design," Appl. Opt. **34,** 1053–1058 (1995).
10. D. L. Brundrett, T. K. Gaylord, and E. N. Glytsis, "Polarizing mirror/absorber for visible wavelengths based on a silicon subwavelength grating: design and fabrication," Appl. Opt. **37,** 2534–2541 (1998).
11. J. M. Miller, N. de Meaucoudrey, P. Chavel, J. Turunen, and E. Cambril, "Design and fabrication of binary trapezoidal surface-relief gratings for a planar optical interconnection," Appl. Opt. **36,** 5717–5727 (1997).
12. R. T. Chen, L. Lin, C. Choi, Y. J. Liu, B. Bihari, L. Wu, S. Tang, R. Wickman, B. Picor, M. K. Hibbs-Brenner, S. Bristow, and Y. S. Liu, "Fully embedded board-level guided-wave optoelectronics interconnects," Proc. IEEE **88,** 780–793 (2000).
13. Y. Li, D. Chen, and C. Yang, "Sub-microns period grating couplers fabricated by silicon mold," Opt. Laser Tech. **33,** 623–626 (2001).
14. M. Okano, H. Kikuta, Y. Hirai, K. Yamamoto, and T. Yotsuya, "Optimization of diffraction grating profiles in fabrication by electron-beam lithography," Appl. Opt. **43,** 5137–5142 (2004).
15. M. G. Moharam and T. K. Gaylord, "Diffraction analysis of dielectric surface-relief gratings," J. Opt. Soc. Am **72,** 1385–1392 (1982).
16. K. Yokomori, "Dielectric surface-relief gratings with high diffraction efficiency," Appl. Opt. **23,** 2303–2310 (1984).
17. M. C. Gupta and S. T. Peng, "Diffraction characteristics of surface-relief gratings," Appl. Opt. **32,** 2911–2917 (1993).
18. H. J. Gerritsena and M. L. Jepsen, "Rectangular surface-relief transmission gratings with a very larger first-order diffraction efficiency (~95%) for unpolarized light," Appl. Opt. **37,** 5823–5829 (1998).
19. S.-D. Wu, T. K. Gaylord, J. S. Maikisch, and E. N. Glytsis, "Optimization of anisotropically etched silicon surface-relief gratings for substrate-mode optical interconnects," Appl. Opt. **45,** 15–21 (2006).
20. S. Kirkpatrick, C. D. Gelatt, and M. P. Vecchi, "Optimization by simulated annealing," Science **220,** 671–680 (1983).
21. A. Corana, M. Marchesi, C. Martini, and S. Ridella, "Minimizing multimodal functions of continuous variables with the simulated annealing algorithm," ACM Trans. Math. Software **13,** 262–280 (1987).